Amphiphilic Helical Peptide Enhances the Uptake of Single-Walled Carbon Nanotubes by Living Cells

Shook-Fong Chin,* Ray H. Baughman,*,† Alan B. Dalton,‡ Gregg R. Dieckmann,*,†,§ Rockford K. Draper,*,†,§,|| Carole Mikoryak,|| Inga H. Musselman,*,† Vasiliki Z. Poenitzsch,* Hui Xie,* and Paul Pantano*,†,§,[1]

*Department of Chemistry and †The NanoTech Institute, University of Texas at Dallas, Richardson, Texas 75080; ‡Department of Physics, University of Surrey, Guildford, Surrey GU2 7XH, United Kingdom; §The Institute of Biomedical Science and Technology and ||Department of Molecular & Cell Biology, University of Texas at Dallas, Richardson, Texas 75080

The success of many projected applications of carbon nanotubes (CNTs) to living cells, such as intracellular sensors and nanovectors, will depend on how many CNTs are taken up by cells. Here we report the enhanced uptake by HeLa cells of single-walled CNTs coated with a designed peptide termed *nano-1*. Atomic force microscopy showed that the dispersions were composed of individual and small bundles of nano-1 CNTs with 0.7- to 32-nm diameters and 100- to 400-nm lengths. Spectroscopic characterizations revealed that nano-1 disperses CNTs in a non-covalent fashion that preserves CNT optical properties. Elemental analyses indicated that our sample preparation protocol involving sonication and centrifugation effectively eliminated metal impurities associated with CNT manufacturing processes. We further showed that the purified CNT dispersions are taken up by HeLa cells in a time- and temperature-dependent fashion, and that they do not affect the HeLa cell growth rate, evidence that the CNTs inside cells are not toxic under these conditions. Finally, we discovered that ~6-fold more CNTs are taken up by cells in the presence of nano-1 compared with medium containing serum but no peptide. The fact that coating CNTs with a peptide enhances uptake offers a strategy for improving the performance of applications that require CNTs to be inside cells. Exp Biol Med 232:1236–1244, 2007

This work was supported by Robert A. Welch Foundation grants AT-1364 (P.P.), AT-1326 (I.H.M.), and AT-0026 (R.H.B.); the Human Frontier Science Program grant RGY0070/2005-C (A.B.D. and G.R.D.); the National Science Foundation (NIRT award DMI-0609115 to R.H.B.); and a gift from the von Ehr Foundation (R.K.D.).

[1] To whom correspondence should be addressed at Department of Chemistry, The University of Texas at Dallas, Richardson, TX 75083-0688. E-mail: pantano@utdallas.edu

Received December 2, 2006.
Accepted May 9, 2007.

DOI: 10.3181/0612-RM-284
1535-3702/07/2329-1236$15.00

Key words: bionanotechnology; nanoparticles; drug delivery; Raman spectroscopy; HeLa cells

Introduction

Nanoparticles functionalized with peptides and peptidomimetics are finding increased utility in biomedical applications involving living cells. For example, Chen and Gerion used SV40 nuclear localization signal (NLS) peptides to functionalize quantum dots (QDs) in order to target them to the nuclei of HeLa cells (1). Vu *et al.* conjugated the peptide ligand βNGF to QDs to initiate neuronal differentiation in PC12 cells (2). Pantarotto *et al.* demonstrated that carbon nanotubes (CNTs) facilitated the internalization of a peptide subunit of a G-protein in fibroblast cells (3). Pantarotto *et al.* functionalized CNTs with peptide derived from a foot-and-mouth disease virus protein to elicit enhanced antibody responses relative to peptide alone (4).

Peptides are also very effective in dispersing hydrophobic CNTs, which are insoluble in water and tend to bundle together. In particular, Wang *et al.* used phage display to identify peptides with selective affinity for CNTs (5); Pender *et al.* used multifunctional peptides to suspend silica- and titanium-coated CNTs (6); Arnold *et al.* used peptide amphiphiles to disperse and encapsulate CNTs (7); and Bianco and co-workers have covalently derivatized CNTs with peptides to form highly water-soluble derivatives (8, 9).

We have also coated CNTs with various designed peptides to disperse them and provide a surface for interfacing CNTs with biologic molecules (10–17). In one approach, a 29–amino acid peptide, designed to fold into an amphiphilic α-helix, was used to coat single-walled CNTs

(10–15). This peptide, termed *nano-1*, disperses CNTs in water as a result of the hydrophobic face of the helix interacting noncovalently with the aromatic surface of CNTs and the hydrophilic face promoting interactions with aqueous environments. Therefore, CNTs coated with nano-1 may provide an interesting model system for presenting CNTs to living cells.

Here we investigate the uptake of nano-1 peptide-coated, single-walled CNTs by cultured mammalian cells. First, the physical and optical properties of CNT dispersions prepared in cell culture media with and without nano-1 were characterized. Next, the purified dispersions were shown to have no effect upon the growth rates of HeLa cells, a thoroughly characterized human epithelial-like cell line. Then, using confocal micro-Raman spectroscopy, it was shown that media-dispersed and nano-1–dispersed CNTs were taken up by cells in a time- and temperature-dependent fashion. Finally, it was discovered that ~6-fold more CNTs were taken up by cells in the presence of nano-1. It is therefore believed that nano-1 and other designed peptides should find future utility as stable, noncovalent scaffolds for attaching ligands and payloads to CNTs for intracellular applications.

Materials and Methods

Media and Solutions. Dulbecco's modified Eagle medium (DMEM) was purchased from Irvine Scientific (Santa Ana, CA). All DMEM solutions were supplemented with 1% (v/v) penicillin, streptomycin, and amphotericin B (Sigma-Aldrich, St. Louis, MO). DMEM supplemented with 5% (v/v) fetal bovine serum (FBS; HyClone, Logan, UT) was used for primary cell culturing and is denoted as *DMEM-1*; it also contained sodium bicarbonate (3700 mg/l) and phenol red (15 mg/l). DMEM-2 also contained 5% (v/v) FBS but did not contain phenol red and sodium bicarbonate; it was used for cell maintenance in the absence of a CO_2 atmosphere and for all optical spectroscopy experiments. DMEM-3 did not contain FBS, phenol red, or sodium bicarbonate; it was used in various sample preparation protocols and control experiments. Phosphate-buffered saline (PBS; 8 m*M* phosphate, 150 m*M* NaCl, pH = 7.4) was sterilized by autoclaving at 120°C for 0.5 hrs. Deionized water (18.3 MΩ-cm) was obtained using a Nanopure Infinity water purification system (Barnstead, Dubuque, IA). All other chemicals were of the highest quality available and were used as received.

Peptide Synthesis. The amino acid sequence of nano-1 using single-letter notation is Ac-E(VEAFEKK)(VAAFESK)(VQAFEKK)(VEAFEHG)-$CONH_2$, where Ac indicates N-terminal acetylation, $CONH_2$ indicates C-terminal amidation, and the parentheses denote heptad repeats (10). Nano-1 was synthesized at a 0.1-mmol scale on an Applied Biosystems (Foster City, CA) 433A solid-phase peptide synthesizer equipped with an Alltech (Deerfield, IL) model 450 UV detector using 9-fluorenylmethoxycarbonyl (Fmoc)-protected amino acids and standard solid-phase peptide synthetic methods as described previously by Dieckmann *et al*. (10). The identity of the pure peptide was verified using electrospray ionization mass spectrometry (HT Laboratories, San Diego, CA). The concentrations of aqueous 1000-μ*M* stock solutions of peptide were validated using a Cary 50 UV-Vis spectrophotometer and a molar absorptivity (ε) of 788 liters mol^{-1} cm^{-1} at 254 nm (10). A variety of 100-μ*M* peptide working solutions were prepared by diluting stock peptide solutions with deionized water or a DMEM formulation.

Single-Walled CNT Dispersions. The preparation of CNT dispersions was similar to that described previously by Zorbas *et al*. (11). The parameters modified were the sonication time and the centrifugation times and speeds; in addition, dispersions were prepared in cell culture media. Specifically, nano-1 peptide-wrapped CNT dispersions (P-CNTs) were prepared by dispensing ~1 mg HiPco single-walled CNTs (32 wt-% metals; Carbon Nanotechnologies Inc., Houston, TX) into an Eppendorf tube containing 1.0 ml of a nano-1 peptide (P) working solution in FBS-free DMEM-3. The mixture was vortexed for ~1 min before it was sonicated using a Branson 250 Sonifier (Danbury, CT). The 2-mm diameter probe tip was placed one third of the distance below the surface of the 1-ml dispersion and was sonicated for 10 mins in an ice water bath. The resulting dense, black dispersion was centrifuged in an Eppendorf 5417C centrifuge for 10 mins at 16,000 *g*. The upper 75% of the supernatant was recovered without disturbing the sediment and was placed in a clean tube before a second 10-min centrifugation at 16,000 *g* was performed. The upper 75% of the resulting second supernatant containing ~0.1 mg/ml CNTs was recovered and supplemented with 5% (v/v) FBS to afford P-CNT dispersions. The preparation of ~0.1 mg/ml CNTs dispersed in DMEM-2 with 5% FBS (i.e., DM-CNTs, no nano-1 peptide present) was identical to that described above for P-CNT dispersions, except that DMEM-2 was used in place of the peptide solution. The only metals detected in these dispersions by ICP-MS (AnaChem Inc., Allen, TX) were iron (1.6 ppm) and nickel (0.02 ppm). In contrast, ICP-MS of the as-received CNT-containing powder revealed 280,000 ppm iron and 330 ppm nickel.

Atomic Force Microscopy (AFM). AFM was performed in air under ambient conditions using a Digital Instruments Nanoscope III MultiMode scanning probe microscope (Woodbury, NY). Images were acquired in the TappingMode using cantilevers with 0.9 N m^{-1} force constants as described by Musselman and co-workers (11, 18). The preparation of P-CNT dispersions was identical to that described above, except that aqueous working solutions of peptide were employed, and all sonication and centrifugation steps were performed in deionized water. AFM samples were prepared by spin-coating 5 μl of an aqueous second supernatant of P-CNTs onto freshly cleaved muscovite mica (Asheville-Schoonmaker Mica Co., New-

port News, VA) at 700 *g* for 1 min; all samples were dried for 24 hrs in a desiccator prior to imaging.

Cell Culture. Human epithelial-like HeLa cells were obtained from the American Type Culture Collection (Manassas, VA). They were cultured in 100-mm diameter polystyrene tissue culture dishes (Sarstedt, Newton, NC) in DMEM-1 in an incubator at 37°C with 90% air and 10% CO_2. Aseptic conditions were maintained at all times, and DMEM-1 was changed every 2 days. Cells were passaged 1:10 every 4 days upon achieving ~80% confluence.

Population Doubling Time (PDT) Assays. HeLa cells were plated into standard 24-well plates (~1×10^4 cells/well; ~20% coverage) and incubated in DMEM-1 at 37°C with 90% air and 10% CO_2. After 24 hrs, the medium was removed and replaced by 350-μl aliquots of one of the following: a working solution of nano-1 peptide (P) in DMEM-1 (no CNTs); a dispersion of P-CNTs in DMEM-1; or a dispersion of CNTs in DMEM-1 (no peptide). Each group of cells was incubated at 37°C with 90% air and 10% CO_2 for 1–4 days, including DMEM-1 controls without peptide or CNTs. Coulter cell counting was performed on Days 1, 2, and 4 by washing the HeLa cells with sterile PBS before harvesting with trypsin-EDTA (Irvine Scientific). PDTs were determined using the equation $PDT = \ln(N/N_o)/t$, where N_o represents the initial cell number, N represents the final cell number, and t represents the time interval between N_o and N (19). Each group of cells was analyzed in triplicate; one-way ANOVA statistical analyses were performed at a 95% confidence level where $P < 0.05$ was considered significant.

Raman Spectroscopy. Raman spectra were acquired from (i) dispersions of P-CNTs and DM-CNTs, and (ii) HeLa cells incubated in dispersions of P-CNTs or DM-CNTs. Dispersions were dispensed directly into 35-mm, polylysine-coated, glass-bottom "imaging" dishes (MatTek, Ashland, MA) and analyzed at room temperature. For HeLa cell analyses, ~3.5×10^5 cells were seeded into imaging dishes with DMEM-1 and were incubated at 37 °C with 90% air and 10% CO_2. After 24 hrs, the medium was removed, and the cells were rinsed with sterile PBS and then incubated in 1 ml of a P-CNT or DM-CNT dispersion. Following the designated incubation periods at 37°C (or 4°C) in air, the cells were rinsed at least four times with sterile PBS. In some experiments, HeLa cell nuclei were stained with Mayer's hematoxylin (Sigma-Aldrich) for 20 mins at room temperature in air. All spectra were acquired at room temperature from PBS-soaked HeLa cells adhering to the dish. Transmitted white-light images were obtained with a 110-W halogen illumination system and a CCD camera.

All Raman spectra acquisition methods were similar to those described previously (10, 12, 13). In brief, baseline-corrected Raman spectra were acquired using a Horiba Jobin Yvon (Edison, NJ) high-resolution LabRam confocal Raman microscope system. The 632.8-nm laser excitation was provided by a Spectra-Physics model 127 helium-neon laser operated at 35 mW (Mountain View, CA). The laser power at the sample was <5 mW using either a 10× (numerical aperture 0.25) or 50× (numerical aperture 0.50) microscope objective. The entrance slit was 250 μm, and the confocal pinhole was 400 μm; the acquisition time for a 300 cm^{-1} spectral region was 30 secs. Wavenumber calibration was performed using the 520.5 cm^{-1} line of a silicon wafer; the spectral resolution was ~1 cm^{-1}. Spectra were fitted with Lorentzian functions by searching for the minimum number of frequencies that fit the different bands equally well without fixing the positions and widths of the individual peaks (10).

Results and Discussion

Characterization of CNT Dispersions. In this work, as-received HiPco single-walled CNTs were dispersed either in DMEM containing FBS (i.e., DM-CNT dispersions) or in DMEM containing the peptide nano-1, with FBS added later (i.e., P-CNT dispersions). The addition of serum to DMEM was essential to disperse CNTs, as DMEM without either FBS or peptide did not support CNT dispersion. The synthesis and characterization of nano-1 has been detailed previously by Dieckmann and co-workers (10–15). In addition, a sonication and centrifugation protocol that affords individual P-CNTs with diameters that range from 0.9 to 6.9 nm and lengths that range from 0.1 to 7.5 μm has been described previously by Zorbas *et al.* (11). To prepare dispersions enriched with shorter CNTs that might be more readily taken up by cells, the Zorbas *et al.* protocol was modified. In brief, the sonication time was increased to shorten CNT lengths, and the centrifugation times and speeds were reduced to increase CNT concentrations. Figure 1 shows a representative AFM image of a mica surface covered with a dispersion of P-CNTs. Individual and small bundles of P-CNTs were observed with diameters and lengths that ranged from 0.7 to 32 nm and 100 to 400 nm, respectively. Elemental analysis of these dispersions found only background levels of iron and nickel catalysts, indicating that these toxic contaminants were effectively removed by the sonication/centrifugation protocol. Titanium, which could come from the sonicator probe tip, was not detected.

The acquisition and interpretation of Raman spectra of P-CNT dispersions, specifically, nano-1 peptide-wrapped, single-walled HiPco CNTs dispersed in water, have been detailed previously (10, 13). Figure 2 (top) shows the Raman spectrum of an aqueous dispersion of HiPco P-CNTs prepared using the modified sonication and centrifugation protocol. The spectrum clearly shows a number of well-characterized nanotube resonances (20); in particular, the radial breathing modes (RBMs) in the 100–300 cm^{-1} region, the D-band at ~1306 cm^{-1}, the G-band in the 1550–1605 cm^{-1} region, and the G′-band at ~2602 cm^{-1}. There were no major differences between the Raman assignments reported previously for P-CNTs dispersed in water (10, 13) and those observed in Figure 2 (top) using the modified

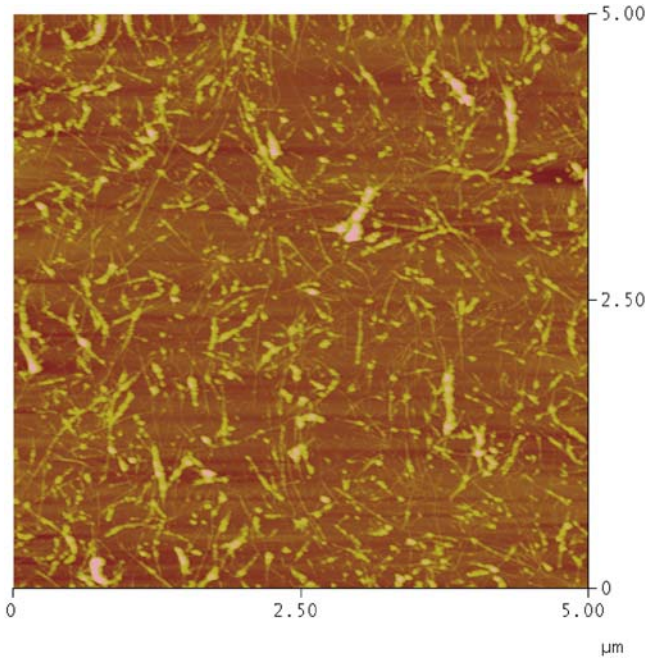

Figure 1. Atomic force microscopy image of an aqueous dispersion of nano-1 peptide-wrapped, single-walled CNTs that was probe-tip sonicated once and centrifuged twice before being cast onto mica.

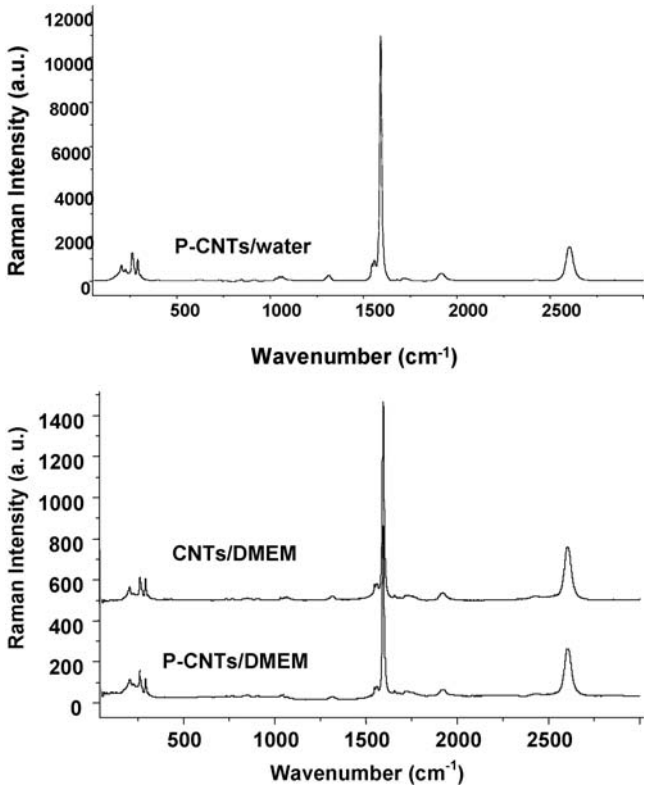

Figure 2. Raman spectra acquired using a 10× objective from a dispersion of P-CNTs prepared in water (top) and of P-CNTs and DM-CNTs prepared in media supplemented with serum (bottom). All dispersions were probe-tip sonicated once and centrifuged twice.

protocol. The Raman spectra of dispersions of P-CNTs and DM-CNTs are shown in Figure 2 (bottom). There were no major differences between the nanotube resonances observed in medium containing serum relative to those observed in water (Figure 2, top). In particular, the peak shapes of the D-, G-, and G′-bands were essentially identical, and three major RBM resonances were observed at 196, 249, and 289 cm^{-1}. Control spectra of DMEM solutions and nano-1 solutions in DMEM (both without CNTs) did not display detectable resonances under these operating conditions (data not shown).

Spectral reproducibility was assessed by monitoring the peak intensity of the G-band at ~1590 cm^{-1}, since it is the most prominent Raman peak indicative of intrinsic single-walled CNT features (21). The relative standard deviation (RSD) of G-band peak intensities acquired from multiple scans of the same region of a DM-CNT dispersion was <1% ($n = 4$; data not shown). The RSD of G-band peak intensities acquired from four different regions of a DM-CNT dispersion was <5% (data not shown), which indicates that the distribution of dispersed CNTs in DMEM-2 was relatively homogeneous. G-band peak intensities were also used to determine relative CNT concentrations. The Raman spectra acquired from a series of dilutions of a DM-CNT dispersion are shown in Figure 3; the plot of G-band peak intensities versus CNT concentrations was linear with a correlation coefficient of 0.990 (data not shown).

Representative absorption spectra of dispersions of P-CNTs and DM-CNTs are shown in Figure 4. The observed van Hove singularities for P-CNT dispersions prepared in media and supplemented with serum were essentially identical to those presented by Zorbas *et al*. for aqueous P-CNT dispersions (11). In general, P-CNT dispersions (prepared in a DMEM/peptide solution with FBS added later) displayed slightly lower absorbance values relative to DM-CNT dispersions (prepared in DMEM and FBS), even though the masses of CNTs used to prepare these dispersions were equivalent. These observations provide indirect evidence that peptide remains associated to CNTs in the presence of FBS. Specifically, if FBS components known to support CNT dispersion (such as bovine serum albumin and phospholipids; Refs. 22–24) displaced peptide, more CNTs would have been dispersed, and equivalent absorbance values for P-CNTs and DM-CNTs should have been observed. In conclusion, both noncovalent approaches share a key advantage in comparison to methods involving the covalent functionalization of CNTs (for reviews, see Refs. 25–28); namely, that covalent approaches introduce defects in the CNT surface that may interfere with the electronic and optical properties of the CNTs that make them so useful.

The Uptake of P-CNTs and DM-CNTs by Living Cells. The main analytical approaches for assessing the presence of CNTs in cells and tissue have been optical (3, 8, 9, 29–35), electron (36–45), and fluorescence (3, 23, 46–54) microscopies. While optical microscopy is ideally suited for

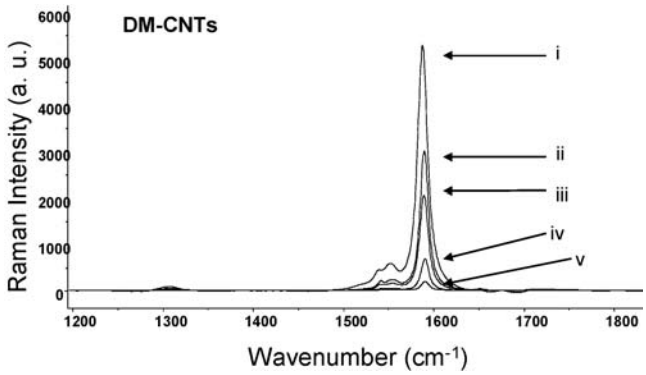

Figure 3. Raman spectra acquired using a 50× objective from a series of dilutions of a CNT dispersion in DMEM-2: (i) the undiluted second supernatant, (ii) diluted 3:4 in DMEM-2, (iii) diluted 1:2, (iv) diluted 1:3, and (v) diluted 1:4. All five spectra were normalized to the same intensity scale.

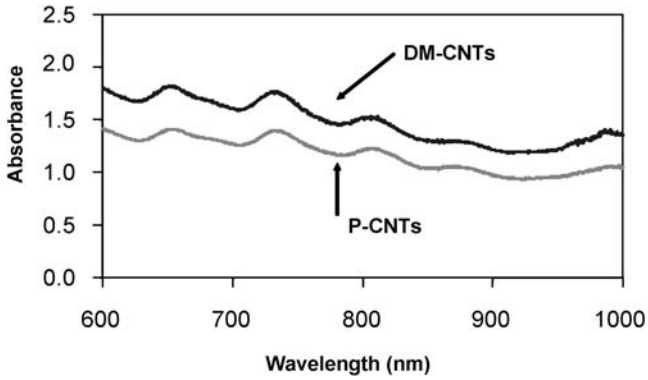

Figure 4. Background-corrected absorption spectra of dispersions of DM-CNTs or P-CNTs; both dispersions were prepared on the same day and were probe-tip sonicated once and centrifuged twice.

live-cell analyses, this label-free technique lacks the specificity to unambiguously identify material observed in cells as CNTs. Electron microscopy offers high spatial resolution imaging of CNTs but is limited to slices of cells that have been fixed; multiwalled CNTs can be unmistakably identified in cells with this technique. In live-cell fluorescence microscopy, the detection of CNTs is indirect (i.e., it is through the detection of a visible fluorescent dye that is (non)covalently attached to the CNT or to molecules coating the CNT). Recently, direct and label-free mapping of CNTs inside living cells have been demonstrated using the intrinsic near-infrared fluorescence (55–57) and Raman scattering (56) of CNTs themselves. Herein, the presence of G-band intensities emanating from living cells incubated in P-CNT or DM-CNT dispersions is evaluated using confocal microRaman spectroscopy.

In the first series of experiments, each culture dish containing $\sim 3.5 \times 10^5$ HeLa cells was incubated in a dispersion of P-CNTs (or DM-CNTs) for 22 hrs at 37°C. An optical micrograph of a live HeLa cell is shown in Figure 5, denoting the typical 15- to 30-μm widths and 40- to 100-μm lengths of these cells. The dimensions of these cells, coupled with the 4-μm lateral resolution of the microprobe system (12), permitted Raman spectra to be acquired from distinct cellular regions. For example, the Raman spectra (D- and G-band regions) acquired from a live HeLa cell that was incubated in a dispersion of DM-CNTs for 22 hrs at 37°C is shown in Figure 5 (top), and that acquired from a different HeLa cell incubated in a dispersion of P-CNTs is shown in Figure 5 (bottom). In both cases, intense G-band signals were observed from the cytoplasm and the nuclear regions, there were no discernable interfering Raman peaks emanating from cellular constituents, and there were no major discrepancies in the spectral profiles acquired from DM-CNTs (or P-CNTs) inside a cell relative to DM-CNTs (or P-CNTs) dispersed in cell culture media (Fig. 2, bottom). Additionally, no detectable CNT resonances were observed from cell-free regions of the dish adjacent (≤ 5 μm) to cells (Fig. 5) or from control cells not exposed to DM-CNTs or P-CNTs (data not shown). In general, the most intense G-bands were recorded from cytoplasmic regions adjacent to the nucleus, but in some cases the G-bands recorded from the nuclear region were greater than those recorded from the cytoplasm, especially cytoplasmic regions at the periphery of these adherent cells where the laser probed a smaller cellular volume. It should be noted, however, that the detection of CNT Raman signatures from a nuclear region does not imply that CNTs are in the nucleus.[1] This is because the detected G-band resonances could emanate from CNTs located in the perinuclear region and/or in the cytoplasm immediately above or below the nucleus. Therefore, for comparative purposes, spectra were acquired from cytoplasmic regions adjacent to the nucleus, and all spectra for a given series of experiments were acquired on the same day to ensure constant Raman operating conditions. Under these conditions, the mean ± SD G-band intensity acquired from cells exposed to DM-CNTs was 342 ± 185 ($n = 6$ measurements from three different cells), and that acquired from cells exposed to P-CNTs was 1983 ± 469 ($n = 6$ measurements from three different cells). Since the absorption spectra for the exact dispersions used in this first series of experiments indicate that the concentration of P-CNTs was slightly lower than the concentration of CNTs dispersed in DMEM with FBS (Fig. 4), the amount of CNTs taken up by cells from P-CNT dispersions was conservatively six times greater than that observed using DM-CNT dispersions that did not contain nano-1.

If the intense G-band signals emanate from CNTs inside cells, most likely as the result of active uptake such as endocytosis, then the signals should be absent in cells exposed to P-CNTs/DM-CNTs at 4°C, where energy-

[1]At present, there is no consensus regarding the ability of CNTs to enter the cell nucleus or how they might be transported there. For example, Strano and coworkers used Raman spectroscopy to observe DNA-coated, single-walled CNTs in the perinuclear zone of 3T3 cells, but not in the nuclear envelope (56), whereas evidence that CNTs have crossed the nuclear membrane has been presented by Pantarotto *et al.* using TEM and 300- to 1000-nm–long, peptide-functionalized, multiwalled CNTs (41) and by Lu *et al.* using radioactive labels and ~400-nm–long, RNA-modified, single-walled CNTs (46).

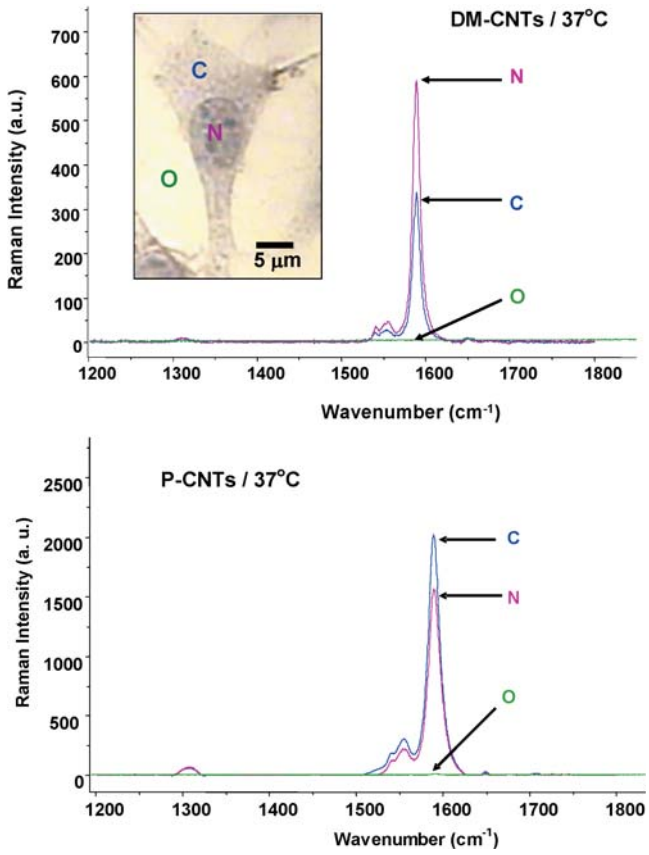

Figure 5. Representative Raman spectra acquired using a 50× objective from live HeLa cells incubated in a dispersion of DM-CNTs or P-CNTs for 22 hrs at 37°C. The spectra were acquired from the cytoplasm (C), the nuclear region (N), and a cell-free region of the culture dish ~2 μm away from the cell (O). (Top) Raman spectra acquired from a single HeLa cell incubated in DM-CNTs. All three spectra were normalized to the same intensity scale. (Bottom) Representative Raman spectra acquired from a different HeLa cell incubated in P-CNTs. All three spectra were normalized to the same intensity scale. (Inset) Representative transmitted white-light image of a HeLa cell stained with Mayer's hematoxylin after incubation in P-CNTs for 22 hrs at 37°C.

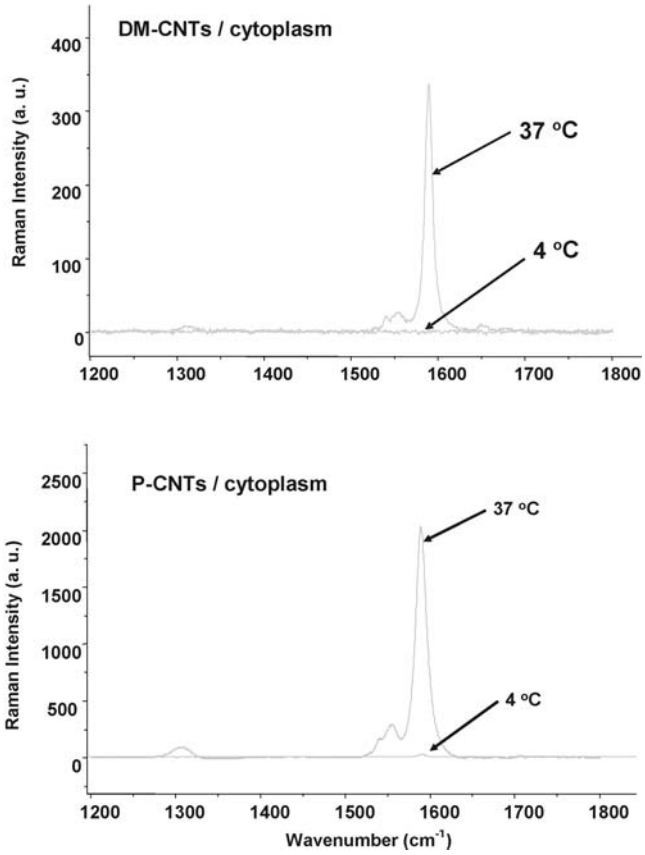

Figure 6. (Top) Representative Raman spectra acquired using a 50× objective from the cytoplasm of two different live HeLa cells incubated in DM-CNTs for 22 hrs at 37°C and 4°C, respectively. Both spectra were normalized to the same intensity scale. (Bottom) Representative Raman spectra acquired using a 50× objective from the cytoplasm of two different live HeLa cells incubated in P-CNTs for 22 hrs at 37°C and 4°C, respectively. Both spectra were normalized to the same intensity scale.

dependent uptake practically ceases. The Raman spectra acquired from the cytoplasms of live HeLa cells incubated with P-CNTs (or DM-CNTs) for 22 hrs at 4°C are shown in Figure 6. In both cases, the intensities of the G-bands recorded at 4°C were less than 98% of those recorded from cells incubated with the exact same dispersions at 37°C ($n =$ 12 measurements from six different cells). This indicates that HeLa cells do not uptake detectable amounts of P-CNTs/DM-CNTs at 4°C. Furthermore, the lack of resonances detected from cells after incubation with P-CNTs/DM-CNTs at 4°C indicates that the nonspecific adherence of P-CNTs/DM-CNTs to HeLa cells was negligible (i.e., the rinsing procedures were sufficient to remove any P-CNTs/DM-CNTs that were merely resting on top of a cell).

In a final series of Raman/cell experiments, the time dependence of CNT uptake was investigated. The G-band intensities acquired from the cytoplasm of HeLa cells incubated in a dispersion of P-CNTs for 22 hrs were 89% greater than those observed from the cytoplasm of cells exposed to P-CNTs for 10 hrs ($n = 3$ measurements from three different cells; data not shown). Similarly, the G-band intensities acquired from the cytoplasm of HeLa cells incubated at 37°C in a dispersion of DM-CNTs for 22 hrs was 91% greater than that observed from the cytoplasm of cells exposed to DM-CNTs for 10 hrs ($n = 3$ measurements from three different cells; data not shown).[2] In summary, the combined Raman evidence indicates that the observed G-band intensities emanate from CNTs inside HeLa cells, that the uptake of P-CNTs and DM-CNTs by HeLa cells is a time- and temperature-dependent process, and that nano-1 enhances the amount of CNTs taken up by cells by ~6-fold.

Cell Growth Rates. A crucial question among reports concerning the adherence and/or uptake of CNTs by cultured cells (3, 8, 9, 23, 29–65) is whether CNTs are

[2]Preliminary confocal fluorescence microscopy studies of live cells incubated at 37°C with a dispersion of P-CNTs prepared using fluorescein-labeled nano-1 have indicated that CNT uptake increases in a linear fashion over the course of 1 day. In association with experiments performed with fluorescein-labeled nano-1 (without CNTs) at 37°C and 4°C, preliminary observations provide evidence that peptide remains associated with CNTs in the presence of FBS and inside cells.

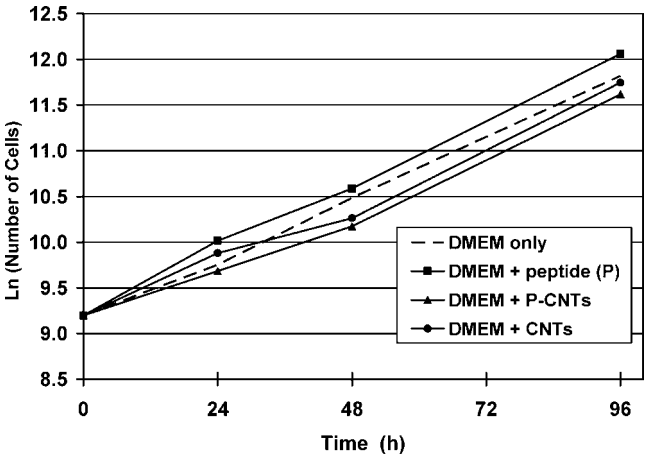

Figure 7. Growth curves for HeLa cells incubated in cell culture media (DMEM-1), DMEM-1 with nano-1 peptide (P), or dispersions of DM-CNTs or P-CNTs.

toxic. To test this, we performed population doubling time (PDT) assays to assess the growth rates of HeLa cells continuously exposed to dispersions of P-CNTs and DM-CNTs. A PDT is a measure of cell number at the early log growth phase and is used for comparisons of normal cell growth. PDTs were obtained from the slopes of the lines of a plot of natural log of cell number versus time (19). Figure 7 shows a representative plot over a time period of 4 days for control cells (no additions) and cells cultured in either a nano-1 peptide DMEM-1 solution (P), a P-CNT dispersion, or a DM-CNT dispersion. For all samples, the respective numbers of HeLa cells counted on Days 1, 2, and 4 were statistically similar. The control HeLa cell PDT was 36 hrs. The PDTs of HeLa cells cultured in P, P-CNTs, and DM-CNTs (35, 40, and 38 hrs, respectively) were also statistically similar. Finally, morphologies of HeLa cells incubated in P, P-CNTs, or DM-CNTs (e.g., Fig. 5) were essentially identical to those of controls (i.e., HeLa cells cultured in DMEM-2 only). In summary, the combined evidence demonstrates that the preparations of nano-1 peptide, P-CNTs, and DM-CNTs used in this work did not inhibit HeLa cell proliferation over the course of 4 days, and that these materials are not inherently cytotoxic to HeLa cells.

In conclusion, we have characterized the physical and optical properties single-walled CNTs dispersed in media supplemented with serum (i.e., DM-CNTs) and in media containing the peptide nano-1, with serum added later (i.e., P-CNTs). We have further shown that our purified CNT dispersions are taken up by HeLa cells in a time- and temperature-dependent fashion, and that they do not affect the growth rate of cells, evidence that the CNTs inside cells are not toxic during the observed time period. Finally, we have demonstrated that ~6-fold more CNTs are taken up by cells in the presence of nano-1 compared with medium containing serum but no peptide. This result is significant, because most projected applications of CNTs to living cells (e.g., intracellular sensors and nanovectors) will depend on how many CNTs are taken up by cells. The fact that coating CNTs with a peptide enhances uptake offers a strategy for improving the performance of applications that require CNTs inside cells.

We are grateful for assistance and contributions to this work by Ramzey Abujarour, Kathryn Hartzell, Alfonso Ortiz-Acevedo, and Amy Smith.

1. Chen F, Gerion D. Fluorescent CdSe/ZnS nanocrystal-peptide conjugates for long-term, nontoxic imaging and nuclear targeting in living cells. Nano Lett 4:1827–1832, 2004.
2. Vu TQ, Maddipati R, Blute TA, Nehilla BJ, Nusblat L, Desai TA. Peptide-conjugated quantum dots activate neuronal receptors and initiate downstream signaling of neurite growth. Nano Lett 5:603–607, 2005.
3. Pantarotto D, Briand JP, Prato M, Bianco A. Translocation of bioactive peptides across cell membranes by carbon nanotubes. Chem Comm (Camb) 1:16–17, 2004.
4. Pantarotto D, Partidos CD, Hoebeke J, Brown F, Kramer E, Briand J-P, Muller S, Prato M, Bianco A. Immunization with peptide-functionalized carbon nanotubes enhances virus-specific neutralizing antibody responses. Chem Biol 10:961–966, 2003.
5. Wang S, Humphreys ES, Chung SY, Delduco DF, Lustig SR, Wang H, Parker KN, Rizzo NW, Subramoney S, Chiang YM, Jagota A. Peptides with selective affinity for carbon nanotubes. Nat Mat 2:196–200, 2003.
6. Pender MJ, Sowards LA, Hartgerink JD, Stone MO, Naik RR. Peptide-mediated formation of single-wall carbon nanotube composites. Nano Lett 6:40–44, 2006.
7. Arnold MS, Guler MO, Hersam MC, Stupp SI. Encapsulation of carbon nanotubes by self-assembling peptide amphiphiles. Langmuir 21:4705–4709, 2005.
8. Bianco A. Carbon nanotubes for the delivery of therapeutic molecules. Expert Opin Drug Deliv 1:57–65, 2004.
9. Klumpp C, Kostarelos K, Prato M, Bianco A. Functionalized carbon nanotubes as emerging nanovectors for the delivery of therapeutics. Biochim Biophys Acta 1758:404–412, 2006.
10. Dieckmann GR, Dalton AB, Johnson PA, Razal J, Chen J, Giordano GM, Munoz E, Musselman IH, Baughman RH, Draper RK. Controlled assembly of carbon nanotubes by designed amphiphilic peptide helices. J Am Chem Soc 125:1770–1777, 2003.
11. Zorbas V, Ortiz-Acevedo A, Dalton AB, Yoshida MM, Dieckmann GR, Draper RK, Baughman RH, Jose-Yacaman M, Musselman IH. Preparation and characterization of individual peptide-wrapped single-walled carbon nanotubes. J Am Chem Soc 126:7222–7227, 2004.
12. Dalton AB, Ortiz-Acevedo A, Zorbas V, Brunner E, Sampson WM, Collins S, Razal JM, Yoshida MM, Baughman RH, Draper RK, Musselman IH, Jose-Yacaman M, Dieckmann GR. Hierarchical self-assembly of peptide-coated carbon nanotubes. Adv Funct Mat 14: 1147–1151, 2004.
13. Xie H, Ortiz-Acevedo A, Zorbas V, Baughman RH, Draper RK, Musselman IH, Dalton AB, Dieckmann GR. Peptide cross-linking modulated stability and assembly of peptide-wrapped single-walled carbon nanotubes. J Mat Chem 15:1734–1741, 2005.
14. Zorbas V, Smith AL, Xie H, Ortiz-Acevedo A, Dalton AB, Dieckmann GR, Draper RK, Baughman RH, Musselman IH. Importance of aromatic content for peptide/single-walled carbon nanotube interactions. J Am Chem Soc 127:12323–12328, 2005.
15. in het Panhuis M, Gowrisanker S, Vanesko DJ, Mire CA, Jia H, Xie H, Baughman RH, Musselman IH, Gnade BE, Dieckmann GR, Draper RK. Nanotube network transistors from peptide-wrapped single-walled carbon nanotubes. Small 1:820–823, 2005.

16. Ortiz-Acevedo A, Dieckmann GR. Synthesis of reversible cyclic peptides. Tetrahedron Lett 45:6795–6798, 2004.
17. Ortiz-Acevedo A, Xie H, Zorbas V, Sampson WM, Dalton AB, Baughman RH, Draper RK, Musselman IH, Dieckmann GR. Diameter-selective solubilization of single-walled carbon nanotubes by reversible cyclic peptides. J Am Chem Soc 127: 9512–9517, 2005.
18. Poenitzsch VZ, Musselman IH. Atomic force microscopy measurements of peptide-wrapped single-walled carbon nanotube diameters. Microsc Microanal 12:221–227, 2006.
19. Martin BM. Tissue Culture Techniques. Boston: Birkhauser; 1994.
20. Dresselhaus MS, Dresselhaus G, Jorio A, Souza Filho AG, Saito R. Raman spectroscopy on isolated single wall carbon nanotubes. Carbon 40:2043–2061, 2002.
21. Itkis ME, Perea DE, Jung R, Niyogi S, Haddon RC. Comparison of analytical techniques for purity evaluation of single-walled carbon nanotubes. J Am Chem Soc 127:3439–3448, 2005.
22. Lin Y, Allard LF, Sun YP. Protein-affinity of single-walled carbon nanotubes in water. J Phys Chem B 108:3760–3764, 2004.
23. Kam NWS, O'Connell M, Wisdom JA, Dai H. Carbon nanotubes as multifunctional biological transporters and near-infrared agents for selective cancer cell destruction. Proc Natl Acad Sci U S A 102:11600–11605, 2005.
24. Karajanagi SS, Yang H, Asuri P, Sellitto E, Dordick JS, Kane RS. Protein-assisted solubilization of single-walled carbon nanotubes. Langmuir 22:1392–1395, 2006.
25. Tasis D, Tagmatarchis N, Georgakilas V, Prato M. Soluble carbon nanotubes. Eur J Chem 9:4000–4008, 2003.
26. Bahr JL, Tour JM. Covalent chemistry of single-wall carbon nanotubes. J Mat Chem 12:1952–1958, 2002.
27. Tasis D, Tagmatarchis N, Bianco A, Prato M. Chemistry of carbon nanotubes. Chem Rev 106:1105–1136, 2006.
28. Banerjee S, Hemraj-Benny T, Wong SS. Covalent surface chemistry of single-walled carbon nanotubes. Adv Mater Weinheim 17:17–29, 2005.
29. Magrez A, Kasas S, Salicio V, Pasquier N, Seo JW, Celio M, Catsicas S, Schwaller B, Forro L. Cellular toxicity of carbon-based nanomaterials. Nano Lett 6:1121–1125, 2006.
30. Sayes CM, Liang F, Hudson JL, Mendez J, Guo W, Beach JM, Moore VC, Doyle CD, West JL, Billups WE, Ausman KD, Colvin VL. Functionalization density dependence of single-walled carbon nanotubes cytotoxicity in vitro. Toxicol Lett 161:135–142, 2006.
31. Worle-Knirsch JM, Pulskamp K, Krug HF. Oops they did it again! Carbon nanotubes hoax scientists in viability assays. Nano Lett 6: 1261–1268, 2006.
32. Warheit DB, Laurence BR, Reed KL, Roach DH, Reynolds GAM, Webb TR. Comparative pulmonary toxicity assessment of single-wall carbon nanotubes in rats. Toxicol Sci 77:117–125, 2004.
33. Cui D, Tian F, Ozkan CS, Wang M, Gao H. Effect of single wall carbon nanotubes on human HEK293 cells. Toxicol Lett 155:73–85, 2005.
34. Garibaldi S, Brunelli C, Bavastrello V, Ghigliotto G, Nicolini C. Carbon nanotube biocompatibility with cardiac muscle cells. Nanotechnology 17:391–397, 2006.
35. Koyama S, Endo M, Kim YA, Hayashi T, Yanagisawa T, Osaka K, Koyama H, Haniu H, Kuroiwa N. Role of systemic T-cells and histopathological aspects after subcutaneous implantation of various carbon nanotubes in mice. Carbon 44:1079–1092, 2006.
36. Shvedova A, Castranova V, Kisin E, Schwegler-Berry D, Murray A, Gandelsman V, Maynard A, Baron P. Exposure to carbon nanotube material: assessment of nanotube cytotoxicity using human keratinocyte cells. J Toxicol Environ Health A 66:1909–1926, 2003.
37. Elkin T, Jiang X, Taylor S, Lin Y, Gu L, Yang H, Brown J, Collins S, Sun YP. Immuno-carbon nanotubes and recognition of pathogens. Chembiochem 6:640–643, 2005.
38. Lam CW, James JT, McCluskey R, Hunter RL. Pulmonary toxicity of single-wall carbon nanotubes in mice 7 and 90 days after intratracheal instillation. Toxicol Sci 77:126–134, 2004.
39. Kostarelos K, Lacerda L, Partidos CD, Prato M, Bianco A. Carbon nanotube-mediated delivery of peptides and genes to cells: translating nanobiotechnology to therapeutics. J Drug Deliv Sci Technol 15:41–47, 2005.
40. Cai D, Mataraza JM, Qin ZH, Huang Z, Huang J, Chiles TC, Carnahan D, Kempa K, Ren Z. Highly efficient molecular delivery into mammalian cells using carbon nanotube spearing. Nat Methods 2: 449–454, 2005.
41. Pantarotto D, Singh R, McCarthy D, Erhardt M, Briand JP, Prato M, Kostarelos K, Bianco A. Functionalized carbon nanotubes for plasmid DNA gene delivery. Angew Chem Int Ed Engl 43:5242–5246, 2004.
42. Bianco A, Kostarelos K, Prato M. Applications of carbon nanotubes in drug delivery. Curr Opin Chem Biol 9:674–679, 2005.
43. Jia G, Wang H, Yan L, Wang X, Pei R, Yan T, Zhao Y, Guo X. Cytotoxicity of carbon nanomaterials: single-wall nanotube, multi-wall nanotube, and fullerene. Environ Sci Technol 39:1378–1383, 2005.
44. Monteiro-Riviere NA, Nemanich RJ, Inman AO, Wang YY, Riviere JE. Multi-walled carbon nanotube interactions with human epidermal keratinocytes. Toxicol Lett 155:377–384, 2005.
45. Smart SK, Cassady AI, Lu GQ, Martin DJ. The biocompatibility of carbon nanotubes. Carbon 44:1034–1047, 2006.
46. Lu Q, Moore JM, Huang G, Mount AS, Rao AM, Larcom LL, Ke PC. RNA polymer translocation with single-walled carbon nanotubes. Nano Lett 4:2473–2477, 2004.
47. Kam NWS, Dai H. Carbon nanotubes as intracellular protein transporters: generality and biological functionality. J Am Chem Soc 127:6021–6026, 2005.
48. Kam NWS, Jessop TC, Wender PA, Dai H. Nanotube molecular transporters: internalization of carbon nanotube-protein conjugates into mammalian cells. J Am Chem Soc 126:6850–6851, 2004.
49. Lin Y, Zhou B, Martin RB, Henbest KB, Harruff BA, Riggs JE, Guo ZX, Allard LF, Sun YP. Visible luminescence of carbon nanotubes and dependence on functionalization. J Phys Chem B 109:14779–14782, 2005.
50. Bianco A, Kostarelos K, Partidos CD, Prato M. Biomedical applications of functionalized carbon nanotubes. Chem Comm (Camb) 5:571–577, 2005.
51. Wu W, Wieckowski S, Pastorin G, Benincasa M, Klumpp C, Briand JP, Gennaro R, Prato M, Bianco A. Targeted delivery of amphotericin B to cells by using functionalized carbon nanotubes. Angew Chem Int Ed Engl 44:6358–6362, 2005.
52. Chen X, Tam UC, Czlapinski JL, Lee GS, Rabuka D, Zettl A, Bertozzi CR. Interfacing carbon nanotubes with living cells. J Am Chem Soc 128:6292–6293, 2006.
53. Dumortier H, Lacotte S, Pastorin G, Marega R, Wu W, Bonifazi D, Briand JP, Prato M, Muller S, Bianco A. Functionalized carbon nanotubes are non-cytotoxic and preserve the functionality of primary immune cells. Nano Lett 6:1522–1528, 2006.
54. Zhu Y, Ran T, Li Y, Guo J, Li W. Dependence of the cytotoxicity of MWCNTs on the culture medium. Nanotechnology 17:4668–4674, 2006.
55. Cherukuri P, Bachilo SM, Litovsky SH, Weisman RB. Near-infrared fluorescence microscopy of single-walled carbon nanotubes in phagocytic cells. J Am Chem Soc 126:15638–15639, 2004.
56. Heller DA, Baik S, Eurell TE, Strano MS. Single-walled carbon nanotube spectroscopy in live cells: towards long-term labels and optical sensors. Adv Mater Weinheim 17:2793–2799, 2005.
57. Heller DA, Jeng ES, Yeung TK, Martinez BM, Moll AE, Gastala JB, Strano MS. Optical detection of DNA conformational polymorphism on single-walled carbon nanotubes. Science 311:508–511, 2006.
58. Manna SK, Sarkar S, Barr J, Wise K, Barrera EV, Jejelowo O, Rice-Ficht AC, Ramesh GT. Single-walled carbon nanotube induces

oxidative stress and activates nuclear transcription factor-kB in human keratinocytes. Nano Lett 5:1676–1684, 2005.

59. Ding L, Stilwell J, Zhang T, Elboudwarej O, Jiang H, Selegue JP, Cooke PA, Gray JW, Chen FF. Molecular characterization of the cytotoxic mechanism of multiwall carbon nanotubes and nano-onions on human skin fibroblast. Nano Lett 5:2448–2464, 2005.
60. Kagan VE, Tyurina YY, Tyurin VA, Konduru NV, Potapovich AI, Osipov AN, Kisin ER, Schwegler-Berry D, Mercer R, Castranova V, Shvedova AA. Direct and indirect effects of single walled carbon nanotubes on RAW 264.7 macrophages: role of iron. Toxicol Lett 165: 88–100, 2006.
61. Flahaut E, Durrieu MC, Remy-Zolghadri M, Bareille R, Baquey C. Investigation of the cytotoxicity of CCVD carbon nanotubes towards human umbilical vein endothelial cells. Carbon 44:1093–1099, 2006.
62. Chlopek J, Czajkowska B, Szaraniec B, Frackowiak E, Szostak K, Beguin F. In vitro studies of carbon nanotubes biocompatibility. Carbon 44:1106–1111, 2006.
63. Panessa-Warren BJ, Warren JB, Wong SS, Misewich JA. Biological cellular response to carbon nanoparticle toxicity. J Phys Condens Matter 18:S2185–S2201, 2006.
64. Oberdorster G, Maynard A, Donaldson K, Castranova V, Fitzpatrick J, Ausman K, Carter J, Karn B, Kreyling W, Lai D, Olin S, Monteiro-Riviere N, Warheit D, Yang H. Principles for characterizing the potential human health effects from exposure to nanomaterials: elements of a screening strategy. Part Fibre Toxicol 2:8–43, 2005.
65. Lam CW, James JT, McCluskey R, Arepalli S, Hunter RL. A review of carbon nanotube toxicity and assessment of potential occupational and environmental health risks. Crit Rev Toxicol 36:189–217, 2006.